Marine and Petroleum Geology 83 (2017) 26–34

Contents lists available at ScienceDirect

Marine and Petroleum Geology

journal homepage: www.elsevier.com/locate/marpetgeo

Research paper

Carbonate slope morphology revealing sediment transfer from bank-to-slope (Little Bahama Bank, Bahamas)

T. Mulder [a, *], M. Joumes [a], V. Hanquiez [a], H. Gillet [a], J.J.G. Reijmer [b], E. Tournadour [a], L. Chabaud [a], M. Principaud [a], J.S.D. Schnyder [c], J. Borgomano [d, e], K. Fauquembergue [a], E. Ducassou [a], J. Busson [a, f]

[a] Université de Bordeaux, UMR 5805 EPOC, Avenue Geoffroy St-Hilaire, CS 5023, 33615 Pessac Cedex, France
[b] Department of Sedimentology and Marine Geology, Faculty of Earth and Life Sciences (FALW), Vrije Universiteit Amsterdam, The Netherlands
[c] CSL-Center for Carbonate Research, University of Miami, 4600 Rickenbacker Cswy., 33149 Miami, USA
[d] Géologie des Systèmes et Réservoirs Carbonatés, Université de Provence, 13331 Marseille Cedex 3, France
[e] Total Centre Scientifique et Technique Jean Féger, 64018 Pau Cedex, France
[f] IFPEN, Avenue de Bois-Préau, Rueil-Malmaison, France

ARTICLE INFO

Article history:
Received 26 April 2016
Received in revised form
16 February 2017
Accepted 1 March 2017
Available online 3 March 2017

ABSTRACT

New high-quality multibeam and high-resolution seismic data reveal new observations on sediment transfer and distribution and margin morphometrics in the uppermost slope of Northeastern Little Bahama Bank between 20 and 300 m water depth. The echofacies/backscatter facies show an alongslope sediment distribution forming successive strips. The upper part of the uppermost slope corresponds to the alternation of several submerged coral terraces and escarpments that could be related to Late Quaternary sea-level variations. The terraces could either be related to periods of stagnating sea-level or slow-down in sea-level change and therefore increased erosion by waves, or periods of accelerated sea-level rise since the Last Glacial Maximum. Terraces could therefore be related to coral construction and drowing. The medium part corresponds to the marginal escarpment, a steep cemented area. The lower part of the uppermost slope shows a discontinuous Holocene sediment wedge with varying thickness between 0 and 35 m. It is separated from the upper part by a zone of well-cemented seafloor associated with the marginal escarpment. Passing cold fronts result in sediment export caused by density cascading. The associated sediment fall-out and convective sedimentation can generate density currents that form this wedge and eventually flow through linear structures on the upper slope. The survey reveals the presence of recently active channels that extend over the entire uppermost slope and interrupt the wedge. The channels connect shallow tidal channels to submarine valleys connected to the proximal part of canyons. They directly feed the canyons with platform-derived sediment forming low-density turbidity currents and could supply the deepest part of the system with coarse-grained sediment directly exported from the carbonate platform.

1. Introduction

Tropical coralgal (skeletal dominated) carbonate systems such as those in the Bahamas differ from their siliciclastic counterparts by the nature of their sourcing and sediment distribution: external (river load) for the latter, internal (biogenic productivity and precipitation) for the former (Eberli and Ginsburg, 1987, 1989; Hine et al., 1981; Wilber et al., 1990). Sediment export from tropical coralgal (skeletal dominated) carbonate factories to the adjacent slopes shares several key characteristics: 1) It generally lacks a single point source, except for steep platform edges (Mullins et al., 1984); 2) Sediment export onto the slope occurs mostly during sea-level rise and highstands, when the shallow water areas have their largest extent, and related sediment production is at its maximum (Schlager et al., 1994); 3) Off-bank sediment transport is episodic and controlled by tides, storms, and cascading density currents (Cook and Mullins, 1983; Wilson and Roberts, 1992, 1995).

However, though sediment production on the platform is now

* Corresponding author.
E-mail address: thierry.mulder@u-bordeaux.fr (T. Mulder).

http://dx.doi.org/10.1016/j.marpetgeo.2017.03.002
0264-8172/

well understood (Schlager, 2005) and morphology and deposition along a carbonate slope are well known (Adams and Kenter, 2013), there are still questions to be addressed concerning sediment transport and dispersion from the production area (shelf) to the slope.

In this paper, we show how the shallow-water realm is connected to the canyon heads. In addition, we discuss the processes of sediment transfer along the uppermost slope during the Holocene.

2. Depositional setting, morphometrics and processes

The Bahamian archipelago was chosen for this study primarily because of the large amount of existing data, making the Bahamas the most studied active carbonate platform tropical factory sensu Schlager (2005) in the world (e.g., Ginsburg, 2001) and the foundation of many of the concepts underpinning carbonate sedimentology and stratigraphy. The archipelago consists of a series of shallow-water carbonate banks separated by deep-water basins and is considered an isolated carbonate system forming a fairly pure carbonate sedimentation environment (Traverse and Ginsburg, 1966; Swart et al., 2014). In addition, the archipelago remained tectonically stable since the middle Tertiary (Masaferro and Eberli, 1999).

This study focuses on the western part of the northern leeward margin of Little Bahama Bank (LBB, Fig. 1A). It is bordered by the Florida Straits to the west, the Atlantic Ocean to the east and north, and the Northwest Providence Channel to the south (Fig. 1A). Oceanic circulation at the study site is dominated by the Antilles current flowing to the northwest along the Blake Bahamas Escarpment and north of LBB, where it merges with the Florida Current to form the Gulf Stream (Neumann and Pierson, 1966).

The study area is a seaward carbonate slope facing the open ocean that is subjected to an energetic ocean surge. The adjacent shallow-water carbonate platform shows a discontinuous barrier consisting of rocky islands called “cays”. Reef barriers made of lithified frame-building organisms and oolitic sand shoals are shaped by strong hydrodynamic processes (Harris, 1979; Hine and Neumann, 1977; Reeder and Rankey, 2008, 2009a; Rankey and Reeder, 2011). Some of these shoals such as Lily Bank (Hine, 1977; Rankey et al., 2006) are currently active and consist of skeletal and oolitic grainstones (Enos, 1974).

The barrier is entirely absent in the northwestern part of LBB (Hine and Neumann, 1977). Tidal channels (inlets) separating the cays and shoals dissect the barrier in the eastern part. They are locally named “cuts”. Upslope and downslope of the tidal channels, the drastic decrease of tidal energy allows the formation of small ebb and flood tidal deltas (Reeder and Rankey, 2009b). Tidal currents swipe these channels twice a day. Despite the low amplitude of the tide in this part of the Bahamas (<1 m), the flow restriction accelerates the current velocity within the tidal channels (Rankey et al., 2006). Reeder and Rankey (2009b), published in situ measurements showing that daily tidal currents can exceed 1 m s^{-1}, far above the velocity threshold (0.26 m s^{-1}) to induce motion of oolites (diameter = 0.5 mm) found in tidal deltas. The same authors also showed that the impact of combined storm waves and induced currents induced only minor adjustments in tidal delta morphology. Although the current induced on the seafloor during storms may be substantially larger than daily tidal currents, their short duration (1–2 days) is believed not to impact the sediment transport substantially and finally, the daily in and out motion induced by the flood and ebb currents smooth the effect of storms and re-adjust the tidal delta morphology. Coarse-grained oolites remain trapped in deltas and only the fine-grained mud fraction can be partially exported. In the study area, we observe five tidal channels: from east to west: Cut 1, Cut 2, Cut 3, Roberts Cut, and Cut 4 (Fig. 1B).

Behind the existing barrier, e.g. south of the Abaco Islands chain, a protected lagoon developed where sedimentation is dominated by carbonate mud, i.e., intensively burrowed peloidal wackestone to packstone (Enos, 1974) dominated by aragonite (Neumann and Land, 1975).

Off-bank transport of fine-grained sediment prevails during sea-level highstands along the leeward margins on the west and south margins of LBB (Hine and Neumann, 1977; Hine et al., 1981). It mixes with particles forming along the upper slope and results in deposition of large amounts of fine-grained periplatform ooze along the adjacent slopes (Hine et al., 1981; Wilber et al., 1990; Roth and Reijmer, 2004, 2005; Betzler et al., 2014).

The western part of the LBB slope is dominated by the activity of the Antilles current that built the LBB contourite Drift. Contourite deposits consist of a mixture of biogenic production by organism living in thewater column and sediments exported from the adjacent platform (Mullins et al., 1980; Lantzsch et al., 2007), forming a typical “periplatform ooze” (Schlager and James, 1978; Lantzsch

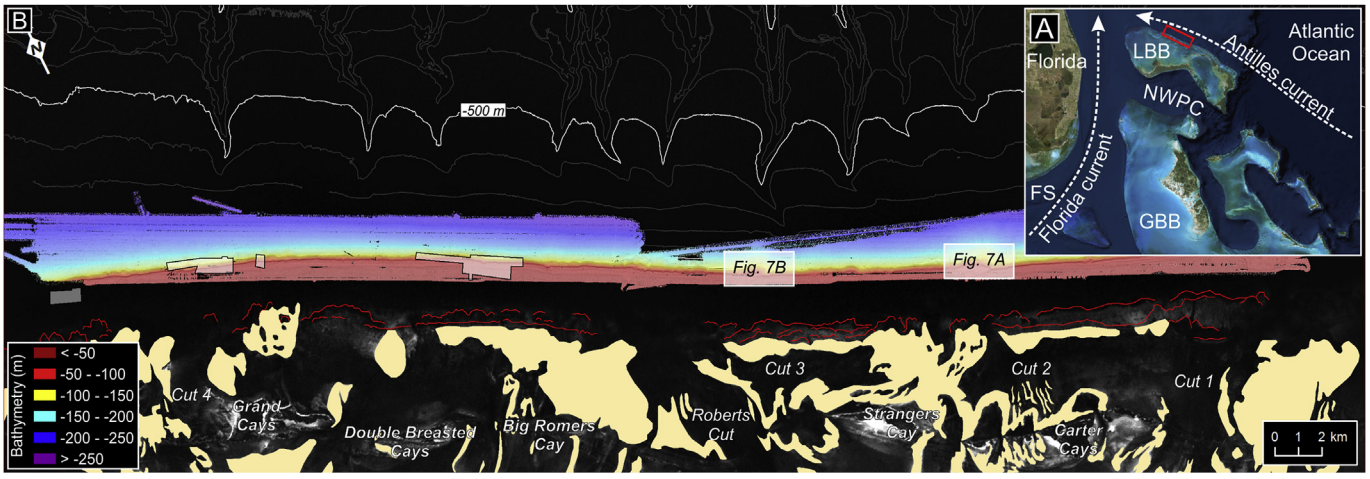

Fig. 1. A: Area covered by the Carambar 1.5 and Carambar cruises (red box). Trajectories of main oceanic currents (white dashed arrows) in the western part of the Bahamian Archipelago. FS: Florida Straits, GBB: Grand Bahama Bank, LBB: Little Bahama Bank, NWPC: Northwest Providence Channel. B: Multibeam bathymetric map obtained during Carambar 1.5 cruise and superposed satellite image showing oolithic shoals (Reeder and Rankey, 2008, 2009a). Transparent black outlined boxes correspond to the AUV multibeam survey sites of Rankey and Doolittle (2012). (For interpretation of the references to colour in this figure legend, the reader is referred to the web version of this article.)

et al., 2007). Additionally, elongated carbonate mounds (lithoherms) have been observed on the western margin of LBB in the Straits of Florida (Neumann et al., 1977). Their distribution was initially related to the presence of seafloor currents providing nutrients (Correa et al., 2012) but recent ROV observations revealed that they were occasionally just carbonate blocks with a light coral cover (Hebbeln et al., 2012).

Recent surveys of the slope adjacent to LBB (Carambar cruise; Mulder et al., 2012) provide new insights to characterise the numerous instability features observed at this location. They have been initially described as gullies or linear canyons by Van Buren and Mullins (1983), Mullins et al. (1984) or Harwood and Towers (1988). New data reveal the accurate morphology of the canyons, feeding turbidite carbonate systems with a length not exceeding 40 km (Mulder et al., 2012). These canyons represent the buried Miocene erosion surface on the LBB and were shaped during this period (Principaud, 2015; Principaud et al., 2016). They spread upward into linear incisions (Tournadour, 2015). The canyons show internal levees that could correspond to sediment accumulated by the spill-over of muddy low-density turbidity currents (Tournadour, 2015). The upper (proximal) part of the canyons extends locally upslope through valleys ending at about 300 m water depth. The amphitheater like shape of the upper part of the canyons shows coalescing slump scars suggesting that they form by backcutting failures. The quite constant bathymetry of the upper part of the valleys suggests that erosion is constrained by the presence of cemented carbonates (Mullins et al., 1985; Puga Bernabéu et al., 2011) that prevent upslope progression of he adward erosion The sediment supply from the shallow-water realms towards the canyons needs further research.

3. Data

The Carambar 1.5 cruise conducted in November 2014 on board the R/V F.G. Walton Smith researched the uppermost slopes of LBB (Fig. 1A). A Teledyne Reson Seabat 7125 multibeam echosounder (bathymetry and acoustic imagery) was used combined with 3.5 kHz echo sub-bottom profiler (Knudsen 3200). A van Veen grab and a 5-m-long gravity corer were used for sediment sampling. Data collected during this cruise include more than 150 km^2 of multibeam bathymetry, 1120 km of high-resolution seismic profiles, and 31 sediment sampling points.

4. Results

4.1. Uppermost slope terraced morphology

The uppermost slope interpretation by Harwood and Towers (1988) and Rankey and Doolittle (2012) was made based on a very small survey surface with multibeam coverage (Fig. 1B). The larger survey surface covered in this study allows interpreting the previously published results with a wider understanding of the morphology at the regional scale. The new bathymetric map shows four terraces (slope flattens locally) and escarpments (slope steepens locally) located between 20 and 100 m present water depth (mpwd, Fig. 2). We focus on the major terraces where the change in slope between terrace and escarpment is well marked, or terraces that are laterally continuous over most of LBB uppermost slope. Terraces and escarpments characteristics are summarized in Table 1. Terrace 1 (t1, Fig. 2) in 22 mpwd is bounded by escarpment 1 (e1, Fig. 2) that extends between 22 and 27 mpwd. Terrace 2 (t2, Fig. 2) between 27 and 33 mpwd t is bordered by escarpment 2 (e2, Fig. 2) that extends between 33 and 40 mpwd. Terrace 3 (t3, Fig. 2) between 40 and 46 mpwd is bounded by escarpment 3 (e3, Fig. 2) that extends between 46 and 55 mpwd. Escarpment 2 and 3 correspond to the 36-m and 48-m escarpment of Rankey and Doolittle (2012), respectively. Terrace 4 (t4, Fig. 2) between 55 and 64 mpwd is bounded by escarpment 4 (e4, Fig. 2), the steepest escarpment that extends between 64 and 96 m with a dip varying between 25 and 50°. The mean dip of escarpment 1, 2, and 3 is 15° and does not exceed 20°. Escarpment 4 corresponds to the marginal escarpment of Rankey and Doolittle (2012) with numerous re-entrants (paleo-inlets) probably caused by small paleo-tidal channels. The escarpment defined by Rankey and Doolittle (2012) at −120 m water depth appears local and does not continue in the surveyed area.

4.2. Upper slope seafloor morphology and sedimentology

The new reflectivity map shows a very sharp gradation in backscatter and associated echofacies in the 3.5 kHz data (Fig. 3A). The backscatter facies distribution is consistent with the echofacies distribution (Fig. 4). Moving downslope from the platform break, one encounters the following sequence: (1) an area with a heterogeneous low backscatter, (2) an area with a high backscatter associated with a blind echofacies, and (3) an area with a homogeneous, moderate-amplitude backscatter associated with a transparent to slightly layered echofacies.

(1) The upper area is located between 20 and 64 mpwd and is bounded by escarpment 4 (marginal escarpment). It shows a heterogeneous low-amplitude backscatter (Fig. 3B and C). Heterogeneity is due to 20 m width patches of low-amplitude backscatter roughly oriented downslope, interfingering with patches of high backscatter. Downslope of the tidal channels, 10 m–50 m width undulating structures with a downslope extent (Fig. 3B) interrupt this backscatter facies and extend over about 300 m, indicating downslope motion of sediment. (2) The intermediate area extends between 64 and 170 to 190 mpwd. It shows homogeneous very high backscatter suggesting a hard-ground, which agrees with the development of the marginal escarpment at this location. It corresponds to a continuous strip of blind echofacies extending parallel to the shelf all along the whole study area with an average width of 1200 m (Fig. 4). Just downslope of the tidal passes, the very high backscatter facies is again interrupted by 40 m width more linear structures still with a rough downslope extent. However, the structures at this location are less well-defined when compared to those observed upslope. The downslope oriented structures correspond to blind echofacies for downslope tidal channels (Fig. 4). Just downslope of this area, between 170 and 190 mpwd and 360 mpwd, homogeneous backscatter with moderate reflectivity (Fig. 3) devoid of sedimentary structures dominates the seafloor. This zone corresponds to the Holocene wedge of Rankey and Doolittle (2012). Fig. 5 shows that the wedge, with thickness ranging from 0 to 35 m (using a sound velocity of 1510 ms^{-1} in subsurface sediments), fills topographic lows in the substratum (Fig. 6). The Holocene wedge recovers unconformably the substratum that is for this reason supposed to be older in age. We assume that the acoustic substratum in Fig. 6 is Pleistocene in age and that the unconformity at the base of the wedge represents a late Pleistocene erosion surface. The reflector at the base of the Holocene wedge could be related to the last glacial maximum or a period of reduced sedimentation enhancing lithification processes (Droxler and Schlager, 1985; Boardman and Neumann, 1984). The wedge corresponds to transparent echofacies passing laterally to layered echofacies (Fig. 6B and A, resp.). The former is present where the wedge is the thinnest and the latter is present where the wedge is the thickest. The wedge is always interrupted downslope of the tidal channels (Figs. 3 and 4). Reflectors show both onlapping and downlapping trends (Fig. 6A) indicative for a highstand wedge rather than a transgressive wedge as was also observed on the

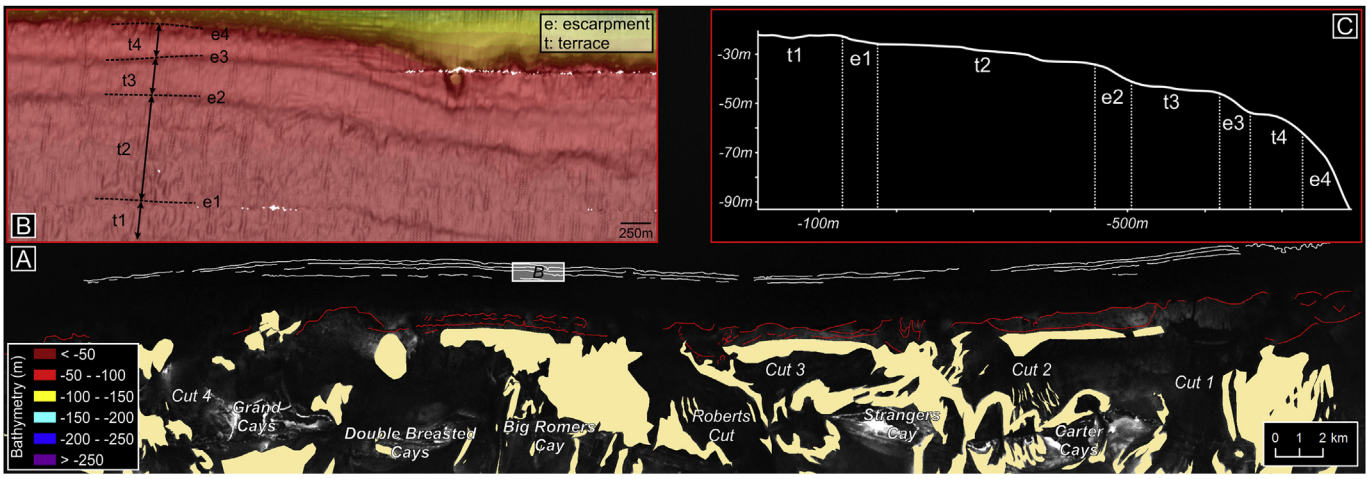

Fig. 2. Morphology of submerged terraces (t1 to t4) and associated escarpments (e1 to e4). A: Lateral extent of the four escarpments separating the terraces along the uppermost slope; B: Bathymetric map showing the detail of terraces and escarpments; C: Bathymetric profile through terraces and escarpments.

Table 1
Main characteristics (bathymetry in metre below present water depth (mpwd), width (m), and mean dip (°) of the morphological features (terraces and escapments) observed on the uppermost slope of the LBB.

Terrace	Escarpment	Water depth (mpwd)	Width (m)	Mean dip (°)
t1		22		
	e1	22–27	≥300	15
t2		27–33	350	1.1
	e2	33–40		15
t3		40–46	140	2.9
	e3	46–55		15
t4		55–64	105	4,5
	e4 (marginal escapment	64–96		25–50

western slope of Great Bahama Bank (Wilber et al., 1990; Roth and Reijmer, 2004; Principaud, 2015). Sediment grabs and cores obtained from this wedge show that it consists of a pteropod/planktonic foram carbonate ooze (wackestone), typical periplatform ooze. The moderate-amplitude backscatter of the Holocene wedge is interrupted downslope by the areas showing undulating downslope structures. They also correspond to topographic highs with an elevation of 30 m above the surrounding mean seafloor on the bathymetric map (Figs. 6 and 7). High-amplitude backscatter associated with a blind echofacies on these topographic high suggest very-indurated seafloor (Fig. 6A). The wedge fills the topographic highs, suggesting they are pre-Holocene. A little channel is present in the eastern part of each high (Fig. 6A and B and 7). Each channel starts at a water depth less than 20 m and connect to little valleys extending upslope to the amphitheater shaped termination of the canyons. They are typically 200 m large and 15 m deep. At higher water depths, reflectivity data collected during cruise Carambar (Mulder et al., 2012) show linear depressions and sediment waves (Tournadour, 2015) that extend downslope from 375 mpwd (Fig. 3A). The linear structures are 2–3 m deep and 50–100 m wide. Some of them connect to the upper part of the canyons; others are located upslope of canyons interfluves, suggesting that they are not related to headward erosion but rather to downslope erosional processes. All the structures observed within the uppermost and upper slope, including the linear depressions, the upper part of canyons, and small incised valleys developing upslope of canyons, are characterized by low-backscatter on the reflectivity map that appear to be similar to the ones characterizing the Holocene wedge. In addition, the continuity between the linear structures and the wedge suggests that these two once formed by spatially and contemporaneously continuous process.

5. Discussion

Sediment distribution along the LBB uppermost slope as shown in the backscatter and echofacies maps displays two main patterns (Fig. 8): (1) The main backscatter/echofacies running distribution with along slope extent, forming trend of parallel homogeneous backscatter/echofacies running parallel to the platform break following isobaths (strips), and (2), downdip structure disrupting the zones of homogeneous backscatter.

Considering the along slope distribution of backscatter facies, two mains strips are visible that are separated by the marginal escarpment.

(1) Above 64 mpwd, i.e. upslope of the marginal scarp, a first strip of low to moderate backscatter corresponds to the four superposed terraces. We based our interpretation of this first strip on Rankey and Doolittle (2012) who worked on the 120-m terrace, i.e. a terrace located outside this strip. They propose that this terrace represents a sea-level stagnation period related to the Last Glacial Maximum (LGM) escarpment based on its water depth. Considering our dataset, this 120-m terrace is the one with the lesser extent despite the fact that it corresponds to the last sea-level lowstand. This is probably related to the presence of steep slopes that limit the growth of coral buildup (see references in Montaggioni and Braithwaite, 2009). In our study area, the lateral continuity of terraces and escarpments and their constant water depth suggest that they are related to sea-level changes rather than representing accumulation of debris and erosional structures (Rankey and Doolittle, 2012). In addition, similar terraces or smaller cuts (notches) younger than the LGM terrace are observed in many places in the world. In the Yellow River subaqueous delta (North Yellow Sea), Liu et al. (2004) describe the succession of four terraces in addition to the LGM terrace (103 mpwd, 67 mpwd (dated from Younger Dryas), 33 to 37 mpwd and 10 to 13 mpwd). Three of these terraces lie at a bathymetry very close (difference < 10 m) to the terraces we observe on the uppermost slope of LBB. On the Ebro River's distal prodelta mud deposits, Diaz et al. (1996) describe relict transgressive sands at 60–80 m

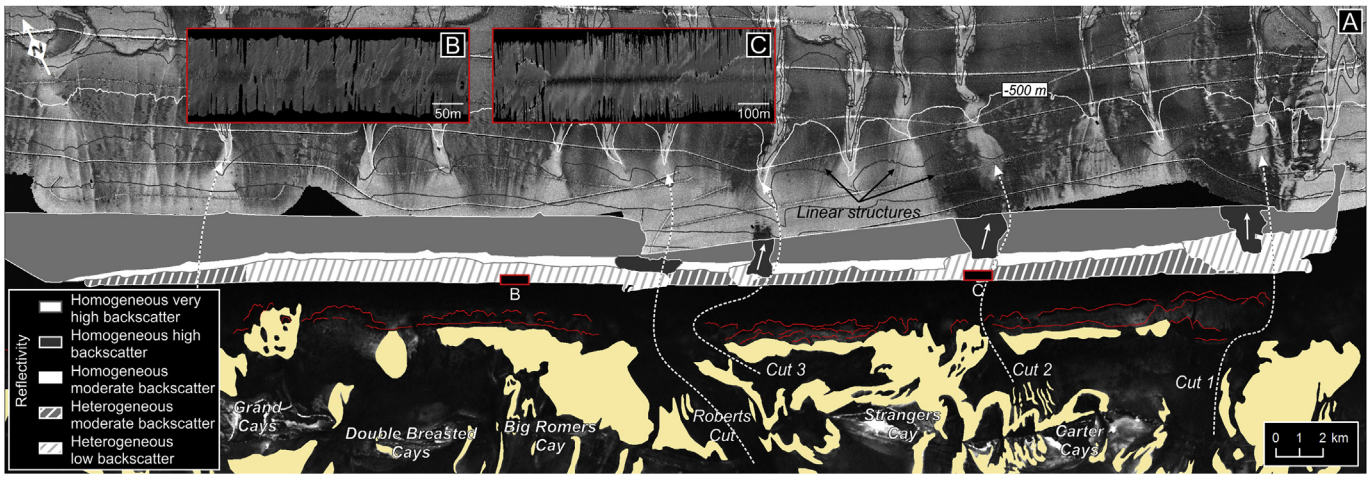

Fig. 3. A: Synthetic backscatter map using the data collected during the Carambar 1.5 cruise and superposed satellite image showing oolithic shoals (Reeder and Rankey, 2008, 2009a); red lines and white dashed arrows correspond to reef barriers and tidal current pathways, respectively. White short arrows correspond to mean slope direction. Isobaths (50 m interval) and backscatter basemap from Carambar cruise (Mulder et al., 2012). B and C: example of heterogeneous low-amplitude backscatter with undulating structures oriented downslope. (For interpretation of the references to colour in this figure legend, the reader is referred to the web version of this article.)

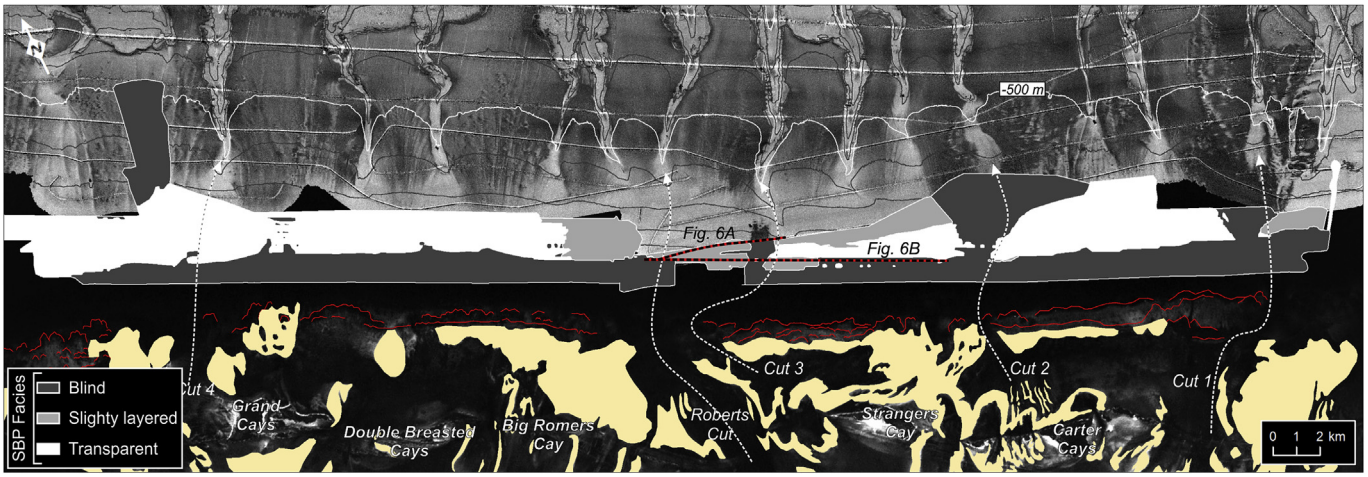

Fig. 4. Echofacies map using the data collected during the Carambar 1.5 cruise.

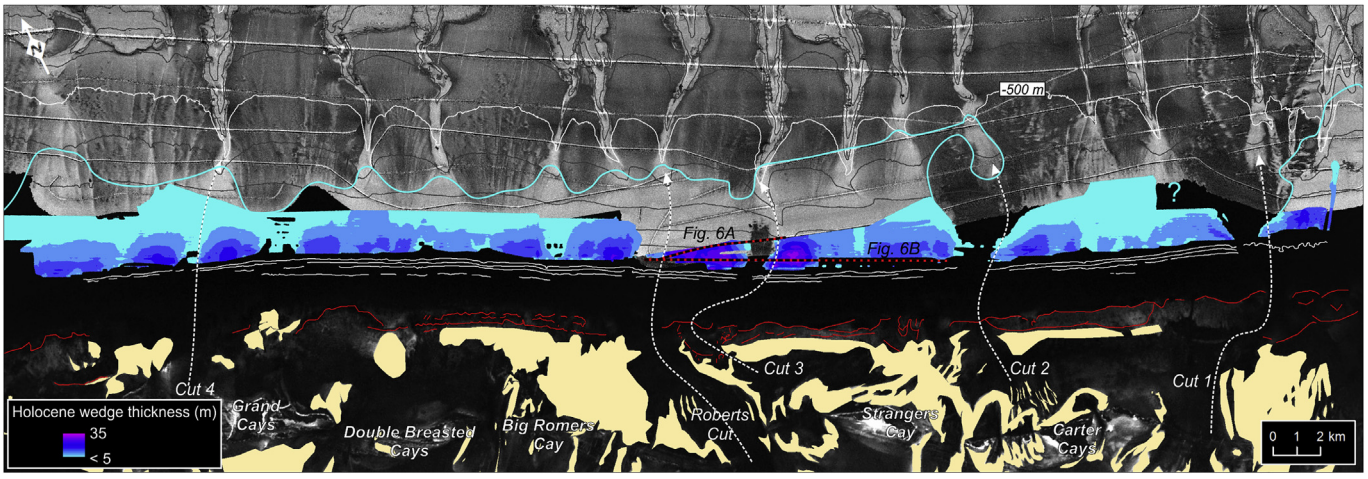

Fig. 5. Isopach map of both transparent and slightly layered echofacies corresponding to the Holocene wedge. Blue lines correspond to Holocene wedge downslope limits. Thin white lines correspond to escarpments bordering the submerged terraces (see Fig. 2 for detail). (For interpretation of the references to colour in this figure legend, the reader is referred to the web version of this article.)

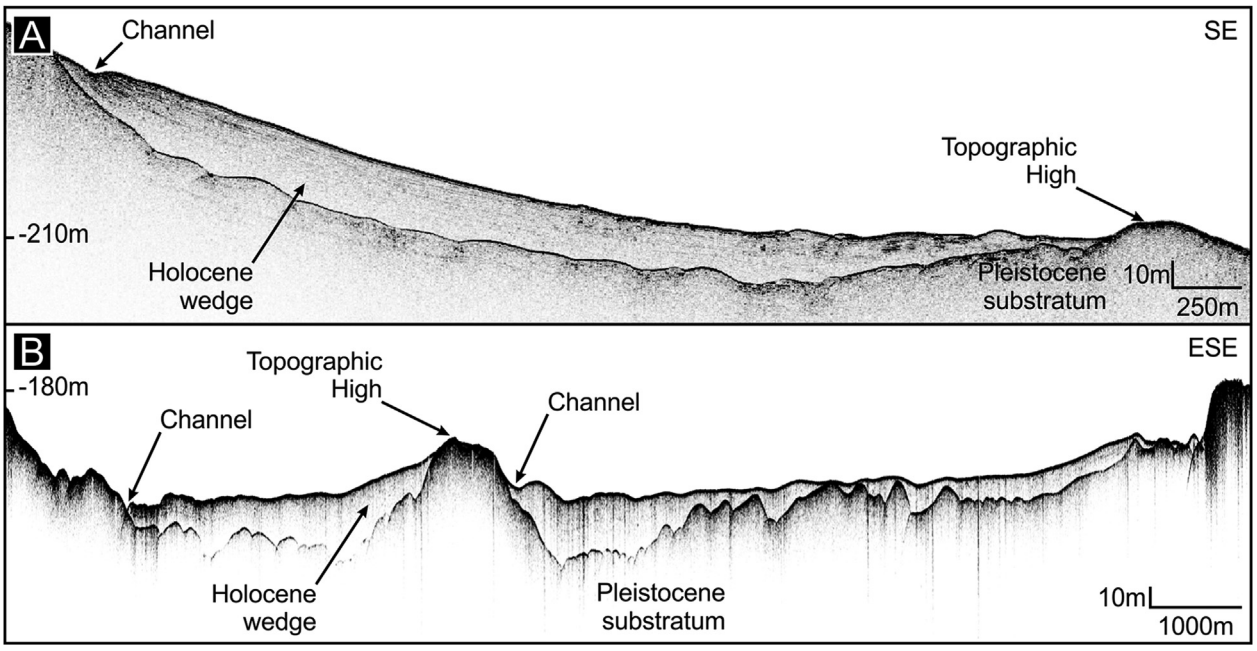

Fig. 6. Sub-bottom profiler seismic line from Carambar cruise showing the onlapping/downlaping geometry and spatial extent of the Holocene wedge. A: Carambar cruise profile. B: Carambar 1.5 cruise profile. See Figs. 5 and 6 for profile location.

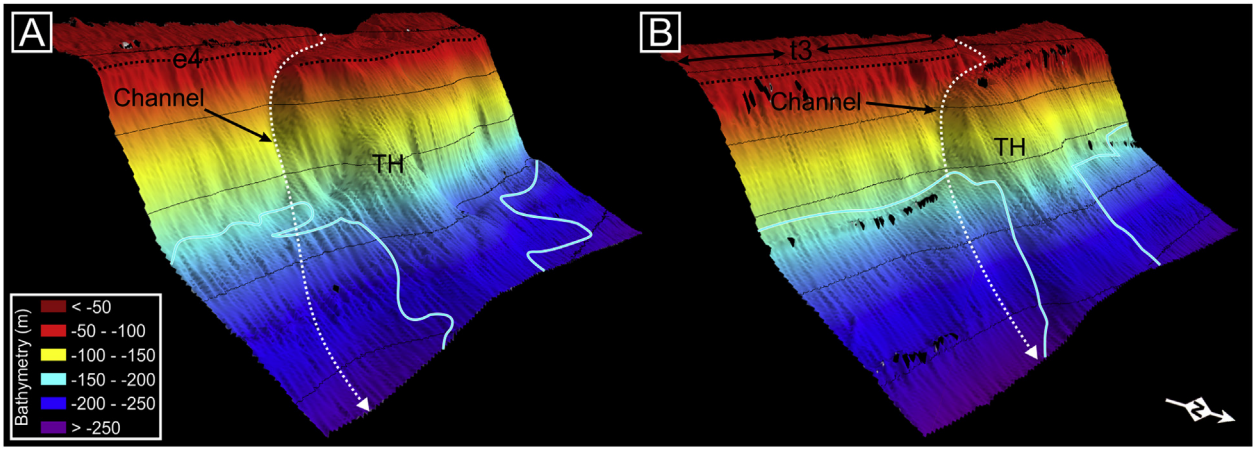

Fig. 7. 3D bathymetry showing the small channels bordering topographic highs (TH) connected to cuts (upslope) and proximal part of canyons (downslope). Black lines represent 50 m equidistant isobaths. Blue lines correspond to Holocene wedge upslope limits. White dashed arrows materialized the sediment transport pathways. t3: terrace 3; e4: escarpment 4. A: Cut 2; B: Cut 3. See Fig. 1 for location. (For interpretation of the references to colour in this figure legend, the reader is referred to the web version of this article.)

water depth (corresponding to our terrace 4) with a ^{14}C age between 10,000–11,000 years. Similar terraces and notches have been described on the shelf edge of the Great Barrier Reef, Australia (Harris and Davies, 1989). On Maldives archipelago, Fürstenau et al. (2010) describe carbonate submerged reef terraces between 55 m and 150 mpwd related either to melt-water pulses or to reef drowning stages. The observed paleomorphology with a series of terraces appears to be very similar to the present-day morphology of the platform edge with very few reefs and topographic highs (shoals and cays) that are interrupted by inlets corresponding to paleo-tidal channels. Their distribution and morphology strongly suggests that the terraces were paleo-platform edges. When they are flat, the terraces possibly relate to periods of stillstand or a slow-down in sea-level change combined with phases of coral construction, increased cementation and flattening of the shallow upper part of the shelf due to hydrodynamic processes. The corresponding sea-level would be comparable to the observed water depth of the terraces plus ~5 m, which is the present mean water depth of the carbonate platform. When they are dipping, the terraces could correspond to wave ravinement surfaces caused by energetic erosional processes such as breaking waves in shallow water depth and episodes of reef-drowning (Fürstenau et al., 2010). Considering the results of Liu et al. (2004) and Diaz et al. (1996), terrace 4 could correspond to the Younger Dryas stillstand in sea level if we consider that the LBB has been tectonically stable since the LGM. However, further dating of corals will be necessary as underlined by Harris and Davies (1989) describing Australian terraces and notches that corresponded to several

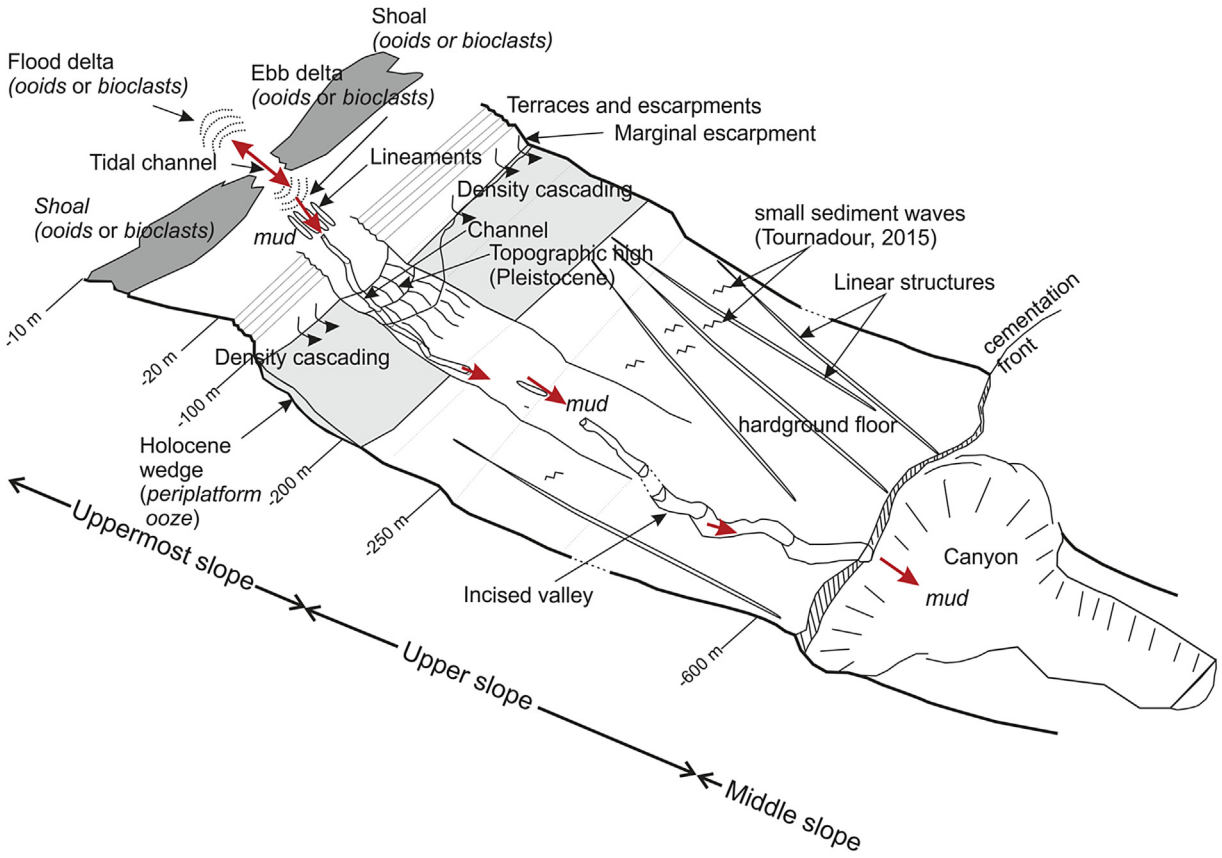

Fig. 8. Synthetic sketch illustrating the sedimentary processes and deposits allowing mud export from the platform to the canyon head at Present-day. Red arrows represent flow velocity vectors. (For interpretation of the references to colour in this figure legend, the reader is referred to the web version of this article.)

superposed Pleistocene sea-level oscillations rather than to a single recent rise in sea level.

(2) Downslope the marginal escarpment, i.e. at a bathymetry exceeding 96 m, the second strip corresponds to the Holocene sediment wedge. The lateral extent of the wedge suggests that it has been deposited by a process acting all along the margin related to large-scale off-bank sediment transport. The cores collected in the wedge show a typical periplatform ooze similar to other Holocene slope oozes (Hine et al., 1981; Rendle and Reijmer, 2002; Roth and Reijmer, 2005; Betzler et al., 2014). Linear structures and sediment waves observed by Tournadour (2015) on the upper slope extend laterally over the entire study area and show a homogeneous moderate backscatter in continuity with the backscatter of the wedge suggesting they consist of the same fine-grained periplatform ooze. At present, fine-grained sediments are produced in protected areas of the platform. Progressive sediment concentration by density cascading (Wilson and Roberts, 1995) can form density- and thus sediment-laden currents at the origin of the linear depressions and the sediment waves observed along the upper slope. This is the most likely way to transport sediment from the shallow platform top to the upper slope, firstly because the barrier prevents most of sediment motion towards the slope, and secondly, this phenomenon only occurs under particular meteorological conditions such as the presence of cold fronts (Wilson and Roberts, 1992, 1995).

The backscatter/echofacies strips are formed by processes acting off the platform, all along the margin, either diagenetic or depositional. The presence of downdip structures perturbs uniformly all the strips of homogenous backscatter/echofacies facies extending alongslope. That suggests this uniform periplatform sediment distribution is perturbed by more energetic downslope processes acting locally. The data set shows that there is a downslope continuity between tidal cuts, high backscatter areas showing undulating or more linear downslope-oriented structures associated with blind/hyperbolic echofacies and channels bordering topographic highs. All these structures are connected together, forming a continuous pathway between the platform and finally connect to small valleys that extend upslope of the proximal part of canyons. All these structures disrupt the lateral extent of the sediment wedge and correspond to areas of high-energy along seafloor sediment transport and a direct downslope transfer of sediment along the seafloor from the platform edge to canyons. These sediment transport pathways are materialized by dashed white arrows in Figs. 3–5 and 7.

The repartitioning of sediment along the uppermost slope suggests two different mechanisms for transport and dispersion.

(1) The first way of sediment transport occurs all along the margin and nourishes the Holocene sediment wedge. The lateral continuity of the wedge suggests that it is fed by a process acting along the entire margin. Density cascading is an active mechanism of sediment dispersion and plunging that has been defined in this area (Wilson and Roberts, 1992, 1995). It represents a pertinent process to explain the emplacement of the wedge. Periods of more intense cascading can explain the development of the linear structure observed downslope of the wedge. This off-bank transport occurs seasonally, when density cascading is active. The second way of sediment transport is related to the channel cuts. These

cuts are local and suggest, conversely to the wedge, a point source for the sediments. The channel cuts enable the present-day export of platform-derived muds directly to the upper slope and through the canyons. In tidal channels, the reduction of the flow section generates an increase of the velocity of the tidal currents (Reeder and Rankey, 2009b). Just downslope of the barrier, the passes enlarge and the coarsest particles settle and form the ebb delta. This sediment export process probably intensifies when hurricanes pass by and suspend sediments produced on the platform similar to the process visible during ebb tides (Neumann and Land, 1975). During these periods lasting a few days at the most during large hurricanes (Reeder and Rankey, 2009b), the muddy fraction of the sediment leaving the tidal passes is flushed downslope and forms the small-scale sedimentary structures (heterogeneous moderate-amplitude backscatter) and the little channels on the uppermost slope. The sediments may form low-concentration sediment flows transporting very fine-grained particles directly into the canyon and may be responsible for confined levees observed in the canyons (Tournadour, 2015).

The channels have been recently active, suggested by the lack of sediments in the deeper parts and because they incise ante-Holocene topographic highs. They provide a pathway through which sediments are directly transported from the platform toward the slope.

This sedimentological and morphological survey allows the reconstruction of a complete and continuous sedimentary profile from the carbonate shelf edge to the uppermost slope (Tournadour, 2015). It provides therefore critical information for the understanding of carbonate sediment transfer from the shallow marine carbonate factory to the slope and deeper environments. The identification of erosive and deposition sedimentary geometries that affect particularly this zone of platform-to-slope transition in response to sea level and hydrodynamics changes, has major impact on carbonate stratigraphic modelling and carbonate seismo-stratigraphic interpretation in ancient analogue carbonate systems. In addition, this study provides new clues concerning the timing of sediment transport along a carbonate margin. It shows that the main type of exported sediment along the Bahamian margin during highstand periods with a fully-flooded platform, such as Holocene, is mainly carbonate mud. However, in some places (tidal passes) the presence of energetic current suggest the potential transport of large particles (bioclasts and oolithes) that could either accumulate in tidal deltas or reach the deepest part of the system (>4000 m water depth) through the Great-Abaco Canyon and form potential good reservoirs.

6. Conclusions

New high-quality backscatter and bathymetry data details the morphology of the uppermost slope of LBB and reveals a complex recent sedimentation history. Four superposed terraces and escarpments are evidenced on the uppermost slope record. The terraces possibly relate to periods of stillstand or a slow-down in sea-level change combined with increased cementation and flattening of the shallow upper part of the shelf due to hydrodynamic processes. The limit between terraces and escarpment could therefore correspond to paleo platform margins. The marginal escarpment corresponds to a highly cemented area (hard-ground). Downslope of this escarpment the Holocene wedge occurs. Most of the present-day sediment export consists of mud, as marked by the occurrence of the highstand wedge. The wedge relates to off-bank transport of the mud formed on the platform mixing with sediments of open ocean origin as deposited along the slope (periplatform ooze). Off-bank export is initiated all along the upper slope when a cold front passes by, resulting in density cascading currents. However, at present, the platform-derived sediments can also be transported downslope in specific areas where a barrier is absent, i.e. between cays and shoals. Tidal energy increases at these positions and density currents can flow through small channels extending along the uppermost slope. The channels transport sediments to submarine valleys on the upper slope, which connect to canyons further downslope. There, the mud load can generate low-density turbidity currents flowing through canyons. Despite the present-day periplatform sedimentation which is dominated by mud, the energy in the tidal passes could be sufficient to export coarser particles to canyons and then to the deepest part of the system located at water depth >4000 m.

Acknowledgments

The authors thank the captain and crew of the RV *Walton Smith* for the quality of the acquired data and the Rosenstiel School of Marine and Atmospheric Sciences for help in cruise organization. Multibeam data acquisition was supervised by Cody Carlson (Seafloor System Inc.). This work is supported by the French INSU program “Actions Marges” and was sponsored by TOTAL Research laboratory. Authors thank J. Kenter and an anonymous revievers for constructive comments on this manuscript.

References

Adams, E.W., Kenter, J.A.M., 2013. So different, yet so similar: comparing and contrasting siliciclastic and carbonate slopes. SEPM Special Publication No. 105. In: Verwer, K., Playton, T.E., Harris, P.M. (Eds.), Deposits, Architecture and Controls of Carbonate Margin, Slope and Basinal Settings. SEPM (Society for Sedimentary Geology), Tulsa, Oklahoma, U.S.A., pp. 14–25

Betzler, C., Lindhorst, S., Eberli, G.P., Lüdmann, T., Möbius, J., Ludwig, J., Schutter, I., Wunsch, M., Reijmer, J.J.G., Hübscher, C., 2014. Periplatform drift: the combined result of contour current and off-bank transport along carbonate platforms. Geology 42, 871–874.

Boardman, M.R., Neumann, A.C., 1984. Sources of periplatform carbonates: northwest Providence channel, Bahamas. J. Sed. Petr. 54, 1110–1123.

Cook, H.E., Mullins, H.T., 1983. Basin margin environment. In: Scholle, P.A., Bebout, D.G., Moore, C.H. (Eds.), Carbonate Depositional Environments. AAPG Memoir 33, pp. 540–617.

Correa, T.B.S., Eberli, G.P., Grasmueck, M., Reed, J.K., Correa, A.M.S., 2012. Genesis and morphology of cold-water coral ridges in a unidirectional current regime. Mar. Geol. 326–328, 14–27.

Diaz, J.I., Palanques, A., Nelson, C.H., Guillen, J., 1996. Morphostructure and sedimentary of the Holocene Ebro prodelta mud belt (northwestern Mediterranean Sea). Cont. Shelf Res. 16 (4), 435–456.

Droxler, A.W., Schlager, W., 1985. Glacial versus interglacial sedimentation rates and turbidite frequency in the Bahamas. Geology 13, 799–802.

Eberli, G.P., Ginsburg, R.N., 1987. Segmentation and coalescence of cenozoic carbonate platforms, northwestern Great Bahama Bank. Geology 15, 75–79.

Eberli, G.P., Ginsburg, R.N., 1989. Cenozoic progradation of NW Great Bahama Bank: a record of lateral platform growth and sea fluctuations. Special Publication. In: Crevello, P.D., et al. (Eds.), Controls on Carbonate Platform and Basin Evolution, vol. 44. SEPM, pp. 339–355.

Enos, P., 1974. Surface Sediment Facies Map of the Florida–Bahamas Plateau. Map. 5. Geological Society of America.

Fürstenau, J., Lindhorst, S., Betzler, C., Hübscher, C., 2010. Submerged reef terraces of the Maldives (Indian ocean). Geo-Marine Lett. 30, 511–515.

Ginsburg, R.N., 2001. Special Publication. Subsurface Geology of a Prograding Carbonate Platform Margin, Great Bahama Bank: Results of the Bahamas Drilling Project, vol. 70. SEPM, Tulsa, Oklahoma, 271 pp.

Harris, P.M., 1979. Facies Anatomy and Diagenesis of a Bahamian Ooid Shoal. Sedimenta, VII. Comparative Sedimentology Laboratory, University of Miami, Miami, pp. 1–161.

Harris, P.T., Davies, P.J., 1989. Submerged reefs and terraces on the shelf edge of the Great Barrier Reef, Australia. Coral Reefs 8, 87–98.

Harwood, G.M., Towers, P.A., 1988. Seismic sedimentological interpretation of a carbonate slope, north margin of Little Bahama Bank. Proc. Odp. Sci. Results 101, 263–277.

Hebbeln, D., Wienberg, C., participants, a.c., 2012. Report and preliminary results of R/V Maria S. Merian cruise MSM20-4. WACOM, West Atlantic Cold-Water Coral Ecosystems: the west side story. Berichte, MARUM – Zentrum für Marine Umweltwissenschaften, Fachbereich Geowissenschaften, Universität Bremen, Bridgetown–Freeport, 14 March–7 April, 2012, p. 120.

Hine, A.C., 1977. Lily Bank, Bahamas; history of an active oolite sand shoal. J. Sediment. Res. 47, 1554–1581.

Hine, A.C., Neumann, A.C., 1977. Shallow carbonate-bank-margin growth and

structure, little Bahama Bank, Bahamas. AAPG Bull. 61, 376–406.
Hine, A.C., Wilber, R.J., Bane, J.M., Neumann, A.C., Lorenson, K.R., 1981. Offbank transport of carbonate sands along open, leeward bank margins: northern Bahamas. Mar. Geol. 42, 327–348.
Lantzsch, H., Roth, S., Reijmer, J.J.G., Kinkel, H., 2007. Sea-level related resedimentation processes on the northern slope of Little Bahama Bank (Middle Pleistocene to Holocene). Sedimentology 54, 1307–1322.
Liu, J.P., Milliman, J.D., Gao, S., Cheng, P., 2004. Holocene development of the Yellow River's subaqueous prodelta, North Yellow sea. Mar. Geol. 209, 45–67.
Masaferro, J.L., Eberli, G.P., 1999. Jurassic-cenozoic structural evolution of the southern great Bahama bank. In: Mann, P. (Ed.), Sedimentary Basins of the World. Elsevier, pp. 167–193.
Montaggioni, L.F., Braithwaite, C.J.R., 2009. Quaternary Coral Reef Systems History, Development Processes and Controlling Factors. Elsevier, Amsterdam v.5, 520 pp.
Mulder, T., Ducassou, E., Eberli, G.P., Hanquiez, V., Gonthier, E., Kindler, P., Principaud, M., Fournier, F., Léonide, P., Billeaud, I., Marsset, B., Reijmer, J.J.G., Bondu, C., Joussiaume, R., Pakiades, M., 2012. New insights into the morphology and sedimentary processes along the western slope of Great Bahama Bank. Geology 40, 603–606.
Mullins, H.T., Neumann, C., Wilber, J., Hine, A.C., Chinburg, S.J., 1980. Carbonate sediment drifts in northern Straits of Florida. AAPG Bull. 64 (10), 1701–1717.
Mullins, H.T., Heath, K.C., van Buren, H.M., Newton, C.R., 1984. Anatomy of a modern open-ocean carbonate slope: northern Little Bahama Bank. Sedimentology 31, 141–168.
Mullins, H.T., Wise, S.W.J., Gardulski, A.F., Hinchey, E.J., Masters, P.M., Siegel, D.I., 1985. Shallow subsurface diagenesis of Pleistocene periplatform ooze: northern Bahamas. Sedimentology 32, 473–494.
Neumann, A.C., Land, L., 1975. Lime mud deposition and calcareous algae in the bight of Abaco, Bahamas: a budget. J. Sediment. Petrol. 45, 763–786.
Neumann, G., Pierson, W.J., 1966. Principles of Physical Oceanography. Prentice-Hall, Inc., Englewood Cliffs, N.J., 545 pp.
Neumann, A.C., Kofoed, J.W., Keller, G.H., 1977. Lithoherms on the Straits of Florida. Geology 5, 4–10.
Principaud, M., 2015. Morphologie, architecture et dynamique sédimentaire d'une pente carbonatée moderne : le Great Bahama Bank (LBB), Bahamas. Ph.D. Thesis. Bordeaux Univ., 307 pp.
Principaud, M., Ponte, J.-P., Mulder, T., Gillet, H., Robin, C., Borgomano, J., 2016. Slope-to-basin stratigraphic evolution of the carbonate northwestern Great Bahama Bank (Bahamas) during the Neogene to Quaternary: interactions between downslope and bottom currents deposits. Basin Res. http://dx.doi.org/10.1111/bre.12195.
Puga-Bernabéu, Á., Webster, J.M., Beaman, R.J., Guilbaud, V., 2011. Morphology and controls on the evolution of a mixed carbonate–siliciclastic submarine canyon system, Great Barrier Reef margin, north-eastern Australia. Mar. Geol. 289, 100–116.
Rankey, E.C., Doolittle, D.F., 2012. Geomorphology of carbonate platform uppermost slope: insights from a Holocene analogue, little Bahama Bank, Bahamas. Sedimentology 59, 2146–2217.
Rankey, E.C., Reeder, S.L., 2011. Holocene oolitic marine sand complexes of the Bahamas. J. Sediment. Res. 81 (1–2), 97–117.
Rankey, E.C., Riegl, B., Steffen, K., 2006. Form, function and feedbacks in a tidally dominated ooid shoal, Bahamas. Sedimentology 53, 1191–1210.
Reeder, S.L., Rankey, E.C., 2008. Interactions between tidal flows and ooid shoals, northern Bahamas. J. Sediment. Res. 78, 175–186.
Reeder, S.L., Rankey, E.C., 2009a. Controls on morphology and sedimentology of carbonate tidal deltas, Abacos, Bahamas. Mar. Geol. 267, 141–155.
Reeder, S.L., Rankey, E.C., 2009b. A tale of two storms: and integrated field, remote sensing, and modeling study examining the impact of hurricanes Frances and Jeanne on carbonate systems, Bahamas. In: Swart, P.K., Eberli, G.P., McKenzie, J.A. (Eds.), Perspectives in Carbonate Geology: A Tribute to the Career of Robert Nathan Ginsburg. John Wiley & Sons, Ltd, pp. 75–90.
Rendle, R.H., Reijmer, J.J.G., 2002. Quaternary slope development of the western, leeward margin of the Great Bahama Bank. Mar. Geol. 185 (1–2), 143–164.
Roth, S., Reijmer, J.J.G., 2004. Holocene Atlantic climate variations deduced from carbonate periplatform sediments (leeward margin, Great Bahama Bank). Paleoceanography 19 (1), PA1003. http://dx.doi.org/10.1029/2003PA000885.
Roth, S., Reijmer, J.J.G., 2005. Holocene millennial to centennial carbonate cyclicity recorded in slope sediments of the Great Bahama Bank and its climatic implications. Sedimentology 52, 161–181.
Schlager, W., 2005. Carbonate sedimentology and sequence stratigraphy. Soc. Econ. Paleontol. Mineral. Concepts Sedimentol. Paleontology no 6, 200 pp.
Schlager, W., James, N.P., 1978. Low-magnesian calcite limestones forming at the deep sea floor, Tongue of the Ocean, Bahamas. Sedimentology 25, 675–702.
Schlager, W., Reijmer, J.J.G., Droxler, A., 1994. Highstand shedding of carbonate platforms. J. Sediment. Res. B64, 270–281.
Swart, P.K., Oehlert, A.M., Mackenzie, G.J., Eberli, G.P., Reijmer, J.J.G., 2014. The fertilization of the Bahamas by Saharan dust: a trigger for carbonate precipitation? Geology 42, 671–674.
Tournadour, E., 2015. Architecture et dynamique sédimentaire d'une pente carbonatée moderne : exemple de la pente Nord de Little Bahama Bank (LBB), Bahamas. Ph.D. Thesis. Université de Bordeaux, 300 pp.
Traverse, A., Ginsburg, R.N., 1966. Palynology of the surface sediments of Great Bahama Bahn, as related to water movement and sedimentation. Mar. Geol. 4, 417–459.
Van Buren, H.M., Mullins, H.T., 1983. Seismic stratigraphy and geologic development of an open-ocean carbonate slope; the northern margin of Little Bahama Bank. In: Sheridan, R.E., Gradstein, F.M. (Eds.), Init. Repts. DSDP, vol. 76. U.S. Govt. Printing Office, Washington, pp. 749–762.
Wilber, R.J., Milliman, J.D., Halley, R.B., 1990. Accumulation of bank-top sediment on the western slope of Great Bahama Bank: rapid progradation of a carbonate megabank. Geology 18, 970–974.
Wilson, P.A., Roberts, H.H., 1992. Carbonate-periplatform sedimentation by density flows: a mechanism for rapid off-bank and vertical transport of shallow-water fines. Geology 20, 713–716.
Wilson, P.A., Roberts, H.H., 1995. Density cascading: off-shelf transport, evidence and implications, Bahama Banks. J. Sediment. Res. A65, 45–56.